Eur Biophys J (1988) 16: 11–21

European Biophysics Journal

Oscillations of electric spatial patterns emerging from the homogeneous state in characean cells

K. Toko, K. Hayashi, T. Yoshida, T. Fujiyoshi, and K. Yamafuji

Department of Electronics, Faculty of Engineering, Kyushu University 36, Fukuoka, 812 Japan

Received June 29, 1987/Accepted in revised form November 17, 1987

Abstract. Electric spatial patterns of bands formed along the cell wall of the characean internode were studied using a multi-electrode measuring system. The electric potential near the surface of the cell was measured by arranging about 25 electrodes along the cell at approximately 1.6 mm intervals. Since the time required for one scan over the cell length is only 1 s, the temporal change in the spatial pattern of surface electric potential can be readily observed. Oscillations were sometimes found as the electric pattern started to appear after the cell was illuminated. Fourier analysis shows that a single spatial mode arises gradually and then becomes stabilized in an oscillatory manner. A simple electric circuit model comprising three variables, i.e., a membrane potential, an electric current across the membrane and an electromotive force, can simulate well the oscillatory rise of bands. These results imply that the electric spatial pattern observed in characean internodes is a self-organized structure emerging far from equilibrium, known as a dissipative structure. Biophysical mechanisms of band formation are discussed.

Key words: Spatial pattern, oscillation, electric potential, self-organization, dissipative structure, *Chara*

Introduction

An internodal cell of *Chara* and *Nitella* develops a banding pattern of surface electric potential along the cell length. It is usually symmetric to the circumferential direction but it is periodic to the longitudinal direction. The periodic spatial pattern is also found for the pH near the cell wall, membrane potential, membrane conductance and often for calcium deposition at the cell wall (Spear et al. 1969; Walker and Smith 1977; Ogata 1983; Ogata et al. 1983; Smith and Walker 1983; Coster et al. 1985). The bands can be considered as a kind of dissipative structure, which is a self-organized structure appearing far from equilibrium (Nicolis and Prigogine 1977). This is suggested by the following experimental facts: *i)* The bands appear from the uniform state along the cell beyond some threshold of light intensity (Ogata 1983), which may be related to the occurrence of proton fluxes from chloroplasts (Hansen 1985). *ii)* Employment of chemicals moves the position of the band (Smith and Walker 1980) and, furthermore, the band will fade under mechanical and electric perturbations (Lucas and Nuccitelli 1980). *iii)* Internodes shorter than 3 mm and young cells rarely show stable bands (Chilcott et al. 1983; Dorn and Weisenseel 1984; Ogata et al. 1987). *iv)* Kinetics of the formation of bands are strongly affected by the volume of the surrounding water phase (Ogata et al. 1987).

Recent theoretical work (Toko et al. 1984, 1985, 1987 a) has reproduced most of these experimental observations. It has been shown that H^+ (or OH^-) circulation appears spontaneously between acidic and alkaline regions when light beyond the threshold level is imposed on the cell. The appearance of high pH values near alkaline regions originates in spatially separated passive H^+ influx (or OH^- efflux) associated with local activation of electrogenic H^+ pumps in acidic regions.

An intimate relationship between the spatial pattern and the oscillation is known for chemical systems coupled with diffusion of reactants and products. In Belousov-Zhabotinskii reactions, a concentration oscillation of products (e.g., Ce^{4+}) appears with retaining spatial homogeneity when the medium is stirred, but many concentration waves of circular type are produced in succession and propagate in the medium without stirring (Nicolis and Prigogine 1977; Smoes 1979). This fact may suggest that the spatial pattern as well as the oscillation is realized through a similar feedback origin. In characean systems, Hansen and coworkers showed the existence of feedback-controlled transport in pH regulation by studying a linearized response of membrane potential to light and

electric current (Hansen 1978, 1980, 1985; Martens et al. 1979; Boels and Hansen 1982; Fisahn et al. 1986). An oscillatory component with a period of several tens of minutes was shown to be inherent although it could barely be seen under constant illumination. However, it sometimes emerged as a self-sustained electric oscillation on changing to low light intensity.

In the present paper, the oscillatory behaviour of the electric spatial pattern is investigated by the use of a multi-electrode measuring apparatus recently developed by us (Toko et al. 1986a). This apparatus is constructed from a maximum of 64 electrodes, a handmade circuit for sampling data and a personal computer for processing and arranging the data. The temporal change in electric potential over the cell length can be detected within an accuracy of several seconds by lining up the electrodes along cell surface with an interval of approximately 1.6 mm. As a result, oscillations were sometimes found when the pattern began to be formed following relatively weak illumination. A sharpening and narrowing phenomenon of the spatial spectrum with growth of a single spatial mode, which is familiar in non-equilibrium systems (Kabashima et al. 1976; Lemarchand and Nicolis 1976), was observed by means of Fourier analysis. To explain the oscillatory rise of the spatial pattern, a simple theoretical model based on electric circuit networks is presented. The observed dynamic behavior was simulated fairly well by an approximate solution of this model. These results may reveal that characean banding is a spatio-temporal organization occurring under far-from-equilibrium conditions, which is related to an ability to generate both the spatial pattern and the oscillation. The biophysical mechanisms of band formation are discussed.

Material and methods

Chara corallina was cultivated in a soil-extract medium in the laboratory. The materials were kindly provided by Dr. Koreaki Ogata. An internodal cell used for experiments was harvested and kept in artificial pond water (APW) at least overnight. The APW contains 0.1 m*M* Na_2SO_4, 0.1 m*M* $CaCl_2$, 0.1 m*M* K_2SO_4 and 0.05 m*M* $MgCl_2$, the pH of which was adjusted to 8.0 using NaOH. Dissolution of CO_2 to the solution was not controlled, because the pH and electric patterns are changed but can appear in the absence of HCO_3^- (Ogata et al. 1987).

The experimental setup of the multi-electrode measuring apparatus is shown in Fig. 1. The details of the apparatus are described elsewhere (Toko et al. 1986a; Hayashi et al. 1987). The internode was laid horizontally on four filter papers in a chamber containing APW. In order to measure an electric potential near the cell surface, about 25 pipette electrodes, which enclosed an Ag/AgCl wire in agar with 100 m*M* KCl, were lined up along the surface of cell wall at a constant separation of 1.6 mm. The tip diameter of the pipette electrode was about 100 μm and the distance between the cell surface and the electrode tip was approximately 1 mm. An electric potential difference between a selected point near the surface and the reference point (Ref in Fig. 1) far from the cell was measured. This configuration of one selected electrode and a reference electrode is similar to the method previously used for measuring the surface potential (Walker and Smith 1977), whereas many electrodes are arranged along the internode in the present experiment.

A measuring electric unit has 64 inputs, each of which is connected to a high input impedance buffer. Its output is selected by analog switches constructed from CMOS switches. The selected signal is amplified, and is converted to digital code by a dual-slope integration A-D converter (Intersil ICL 7109). The time needed for measuring 64 points with this apparatus is about 3 s. Because of this small converting time, the time-course of the pattern can be readily observed. A personal computer (Fujitsu FM-11) was used to control this measuring unit and to process the experimental data.

Experiments were carried out at 28 ± 1 °C in an air-conditioned laboratory. A 60 W incandescent lamp was positioned away from the chamber to illuminate the internode. The light intensity was 13 W m^{-2}. In the case of weak illumination (approximately 4 W m^{-2}),

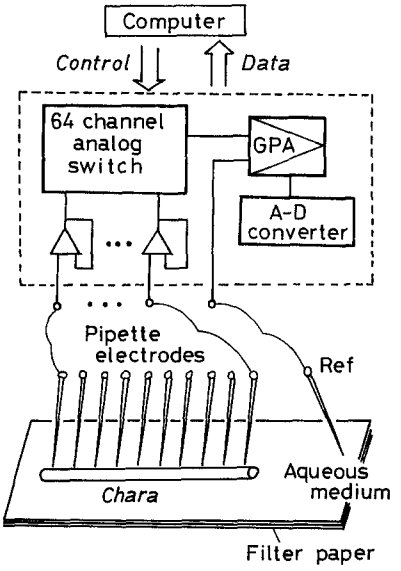

Fig. 1. Experimental setup and multi-electrode measuring system. Pipette electrodes are lined up along the surface of the cell. The outputs are connected to the 64 channel analog switch, and are selected to be processed by the use of a personal computer. A gain programmable amplifier is denoted by GPA. For the internode with, e.g. 32 mm length, 20 electrodes are arranged along at about 1 mm from the surface

the lamp was placed at almost the same height as the chamber so that the light passed through the layer of water surrounding the internode.

The measured potential value is generally accompanied by an offset voltage caused by an input buffer, an amplifier and a pipette electrode. The offset values for individual electrodes were different. Hence zero level adjustment was executed in data processing: These offset values correspond to those measured in the absence of an internode in the experimental chamber. They were eliminated by subtracting them from the potential values measured near the cell surface. The offset voltages were measured after each series of experiments. The resultant potential of 20 electrodes placed in the aqueous medium as a test case showed a zero level with good stability (Toko et al. 1987b). The extrapolation procedure was used for all data on spatial patterns.

A maximum entropy method (MEM) was adopted for spatial spectrum analyses. The data for potential difference along the cell usually showed a gradient from one end of the cell to the other (Ogata et al. 1987). The MEM spectrum was, therefore, computed after the linear trend was eliminated by means of a least-squares fit.

To identify the positions of alkalinization near the surface, the cell was dipped into a solution of 1 m*M* phenol red and 2% methylcellulose adjusted to pH 7.5.

Results

An example of the electric pattern appearing under illumination is given in Fig. 2, the bars indicate the positions of alkalinization. It can be seen that the surface electric potential in these alkaline regions is depolarized compared with neighbouring regions. The electric potential profile and the pH pattern of the internode have a good correlation, as reported previously (Walker and Smith 1977). The electric pattern was usually stable under illumination but it sometimes tended to fluctuate with a period of approximately 12 min under relatively weak light intensity (Hayashi et al. 1987).

The spatial period in Fig. 2 amounts to 3 ~ 8 mm. This is comparable to previous reports concerning calcium deposition, surface pH, surface potential, and membrane potential (Spear et al. 1969; Walker and Smith 1977; Ogata 1983; Coster et al. 1985; Ogata et al. 1983, 1987). In some cases, however, banding with high spatial frequencies can be seen (Ogata 1983; Coster et al. 1985). This may be due to the high resolution of the water-film electrode, which is continuously moved along the cell. In contrast, the present method relies on a discrete arrangement of electrodes and thus acts as a spatial low-pass filter and suppresses the high frequency pattern.

Two examples of spatial patterns under constant illumination are given in Fig. 3 as a function of time. The electric pattern is almost stable but slight changes can be observed at some positions and times. In Fig. 3a, the electric potential around 5 mm decreases drastically at 33 min; in Fig. 3b a distinct change over

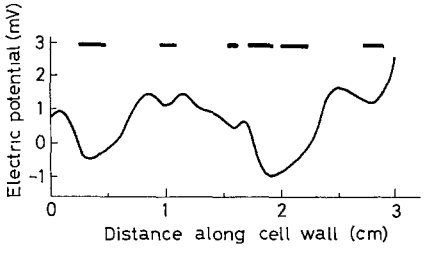

Fig. 2. Example of the spatial pattern of electric potential near the surface of the internodal cell. The bars indicate the positions of alkalinization. The lower-level potential regions correspond to the alkaline regions. The cell length is 32 mm. The light intensity was 13 W m^{-2}

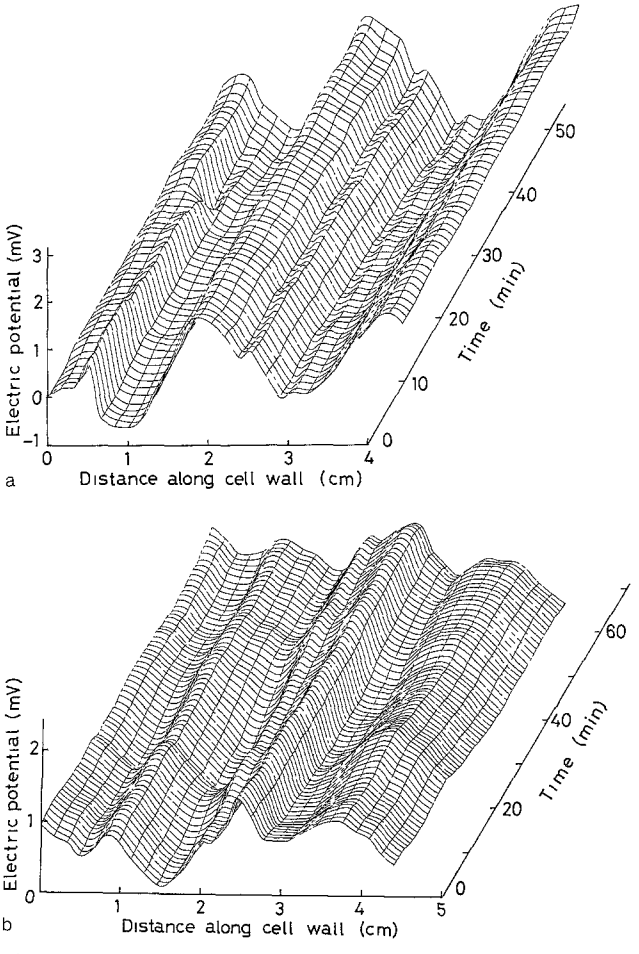

Fig. 3a and b. Two examples of electric spatial patterns as a function of time under constant illumination. The cell lengths are 45 mm (**a**) and 46 mm (**b**). The interval of each scan along the cell is one minute. While the patterns are generally stable, small fluctuations can be seen. The light intensity was 13 W m^{-2}

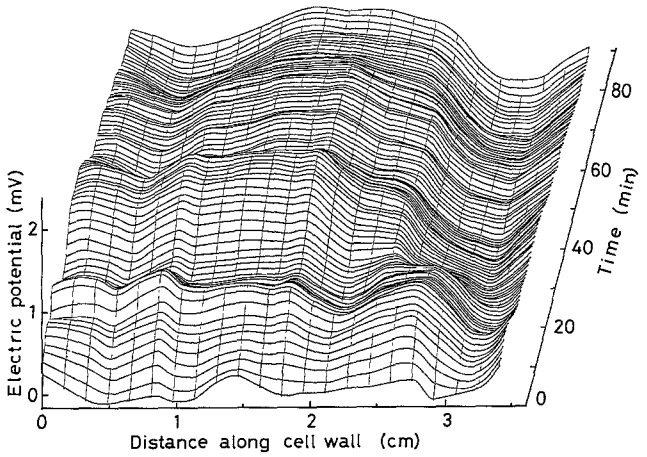

Fig. 4. Formation of the electric spatial pattern accompanying the oscillation after the illumination. The cell length is 36 mm under light intensity of approximately 4 W m^{-2}. Two alkaline regions are formed, first around 28 mm and later around 5 mm

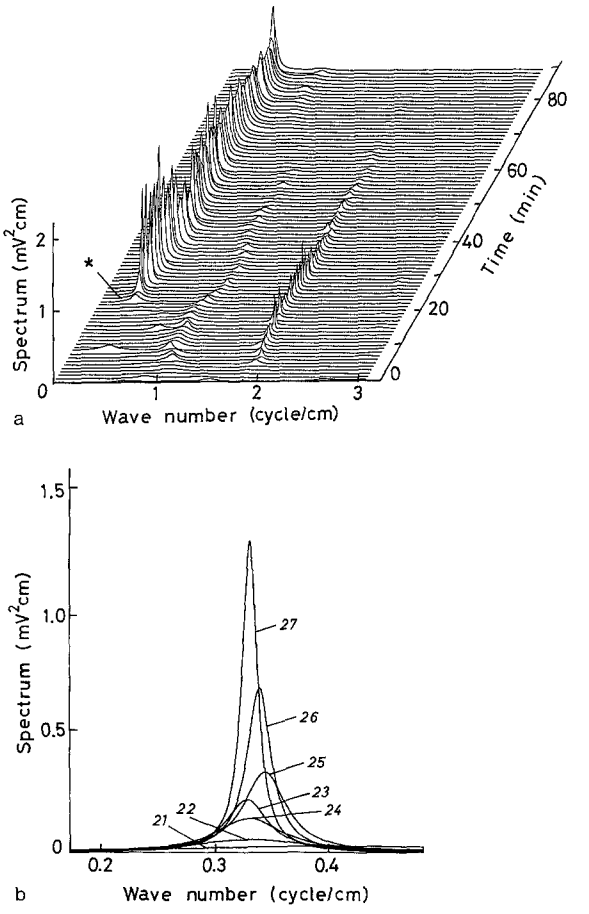

Fig. 5. Spatial power spectrum of rise of spatial pattern with illumination. The data are from Fig. 4. **a** The overall change in spatial spectrum is shown. The peak around 0.35 cycle/cm oscillates periodically, showing the oscillatory formation of electric pattern along the cell. The modes with higher wave numbers decay later. **b** Growth of spatial mode around 0.35 cycle/cm (denoted by an *asterisk* in **a**) is illustrated. The number attached to each curve represents the time (min) from the onset of illumination. The spectrum at 24 min is lower than that at 23 min; this may suggest fluctuation-like behaviour. The spectrum at 27 min is much higher than that at 21 min, implying the formation of a spatial pattern

almost the whole cell length can be seen, for example at about 20 min. A careful inspection of these patterns leads to the conclusion that the pattern of surface electric potential is dynamic, being accompanied by small temporal fluctuations of a few hundred μV during a relatively long span of measurement.

Oscillations can sometimes be seen on forming the electric pattern from the homogeneous state along the cell after the start of weak illumination. The exact experimental conditions that lead to the appearance of oscillations have not been found in the present study. Even under constant illumination, a number of internodal cells showed spontaneous oscillations. Figure 4 shows the oscillations associated with the appearance of the pattern. The overall increase of surface electric potential occurs approximately 20 min after the onset of illumination. This is generally the case in studies of membrane potential (Ogata et al. 1987), where complete hyperpolarization occurs. In the normal case of strong illumination, a decrease in potential follows in some localized regions and they develop into the lower surface electric regions, i.e. the alkaline regions (Hayashi et al. 1987). In Fig. 4 a stable low surface electric region begins to form around 28 mm at approximately 30 min. Other regions also exhibit a decrease in electric potential, but they subsequently show an increase. This process is repeated with a period of approximately 30 min. While a low potential region is also formed around 5 mm, this region shows an oscillation similar to that shown by regions with high electric potential. In this way, the spatial pattern associated with the oscillation appears along the cell.

Figure 5 a shows the rise of the spatial spectrum when the pattern emerges after illumination, the data are from Fig. 4. From this spatial spectrum it can be seen that the spatial mode at 2 cycle/cm (corresponding to a spatial period of 5 mm) appears first after illumination. Subsequently the mode at 0.35 cycle/cm becomes dominant. This mode shows an oscillatory increase, in agreement with Fig. 4. This original mode at 2 cycle/cm eventually decays, leaving only the mode at 0.35 cycle/cm.

Furthermore, the narrowing and sharpening of the spatial spectrum with the 0.35 cycle/cm mode can be seen in Fig. 5 b, which is a magnification of the part shown by an asterisk in Fig. 5 a. This kind of sharpening phenomenon is characteristic of the appearance of a self-organized state under far-from-equilibrium conditions (Lemarchand and Nicolis 1976; Walgraef et al. 1980). A reduction of the band width of the temporal

power spectrum was reported for self-sustained oscillations appearing spontaneously in a Gun diode and squid giant axons, which are not directly related to spatial pattern formation (Kabashima et al. 1976; Matsumoto 1981). The sharpening of the spatial spectrum implies that the spatial coherency is increased along the entire cell length. Existence of coherency can also be demonstrated by a phase-locked giant oscillation along the cell (Hayashi et al. 1987). Thus we can regard electric-pattern formation in the *Characeae* as a typical cooperative phenomenon. Similar coherency can be observed in multicellular systems (Toko et al. 1987b). These phenomena are suggestive of a coherent excitation which has been theoretically predicted (Fröhlich 1983; Webb and Thornton 1985).

Theory

An electric circuit model

In the present section, a mathematical model is presented for simulating the experimental data on the oscillatory rise of the spatial pattern shown in Fig. 4. For this purpose it may be useful to take account of a mathematical model for nerve excitation, namely the FitzHugh-Nagumo model (Nagumo et al. 1962; FitzHugh 1969). Since this model is much simplified, many properties such as self-oscillations and wave propagation can be simulated and also analyzed by the use of a perturbative method (Yamafuji et al. 1981; Toko et al. 1981).

One can illustrate an electric circuit (Fig. 6) of the system composed of the plasmalemma and the intra- and extracellular aqueous media in a similar way to the FitzHugh-Nagumo model. In this model, the electric property of plasmalemma coupled with biophysical steps within the cell is represented by four kinds of electric elements: an electric capacitance C, a resistance R, an inductance L and an electromotive force (emf) E. It is possible to interpret E as the electromotive part of electrogenic H^+ pump. The electric resistance of the extracellular medium is denoted by R_1, which is defined in the region of width Δz with z denoting the longitudinal direction along the cell. Since the electric conductivity in the protoplasma is much higher than that in the extracellular medium, the intracellular resistance is set to zero, as has been done elsewhere (Nagumo et al. 1962; FitzHugh 1969). Let V denote the surface electric potential measured from the inside of the cell and I the electric current across the membrane. The equations for V and I are obtained from Fig. 6:

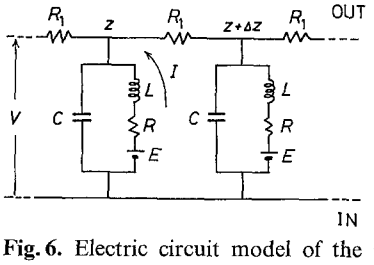

Fig. 6. Electric circuit model of the system composed of the membrane, the intracellular and the extracellular media. The z axis is along the longitudinal direction of the cell. The extracellular electric resistance is designated by R_1. The electric elements C, L, R and E are the electric properties of the membrane. These elements are not directly related to the electrophysiological components of the plasmalemma but include biophysical steps between the electric current across the plasmalemma and activation of reactions in chloroplasts by light. This electric circuit leads to Eq. (1) and (2)

$$C\,\partial V/\partial t - D\,\partial^2 V/\partial z^2 = I, \tag{1}$$

$$L\partial I/\partial t = -V - RI + E, \tag{2}$$

with t the time and D defined by

$$D = (\Delta z)^2/R_1. \tag{3}$$

The efflux across the membrane at z equals $-D\,\partial^2 V/\partial z^2$ in the stationary state, and the longitudinal flow along the cell is given by $-(D/\Delta z)\,\partial V/\partial z$. Equation (1) is the continuity equation holding at the point z in Fig. 6, and Eq. (2) is the balance equation for the potential difference between the intra- and extracellular media across the membrane.

We assume that the electromotive force E is activated through an internal factor e by the following linear relation (see Toko et al. 1985):

$$E = a\,e, \tag{4}$$

where a is the numerical coefficient. It seems natural to adopt the simplest equation of reaction-diffusion type for e:

$$\tau\,\partial e/\partial t - D_1\,\partial^2 e/\partial z^2 = -K_1 V + K_2 e, \tag{5}$$

where τ denotes the characteristic relaxation time expressing a damping process, K_1 and K_2 are the relevant reaction coefficients. The diffusion constant of e is designated by D_1. Equation (5) implies that e is activated through itself, i.e. in a positive-feedback fashion, but is deactivated through the increase in V, which is a suppression effect. The positive feedback origin of the H^+ pump was introduced in our previous work (Toko et al. 1985, 1987a), and is detailed in Figs. 8 and 9. The factor e may be regarded as the internal pH, being the input signal of the pump (Hansen 1980, 1985; Fisahn et al. 1986; Ogata et al. 1987). Substituting Eq. (4) into Eq. (5), we get

$$\partial E/\partial t - d\,\partial^2 E/\partial z^2 = -k_1 V + k_2 E, \tag{6}$$

where d, k_1 and k_2 are

$$d = D_1/\tau, \quad k_1 = K_1 a/\tau, \quad k_2 = K_2/\tau. \tag{7}$$

The set of Eqs. (1), (2) and (6) relates the three variables: surface potential V, electric current I and emf E.

Equations (1) and (2) may be combined to give:

$$\frac{\partial^2 I}{\partial t^2}+\frac{R}{L}\frac{\partial I}{\partial t}+\frac{I}{LC}=\frac{1}{L}\frac{\partial E}{\partial t}-\frac{D}{LC}\frac{\partial^2 V}{\partial z^2}. \tag{8}$$

This equation is similar to that proposed by Hansen (1980, 1985) for explaining the feedback control of the electrogenic pump, except for the addition of the second term on the RHS. Each coefficient is related to a biophysical process. The electric elements L, R and C should be interpreted as quantities which describe the biophysical mechanism for feedback control of the pump, although their biophysical meaning is not so clear as that of Hansen (1980, 1985). The spatial derivative of V included in Eq. (8) comes from the longitudinal flow of H^+ (or OH^-) along the internodal cell between the alkaline and acid regions. This term clearly causes the spatial pattern, the time derivative in Eq. (8) generates the oscillation. The present equation can therefore be considered as a modified one which considers the spatial pattern together with the oscillation investigated previously (Hansen 1980, 1985).

Comparison with observed data

Equations (1), (2) and (6) can be solved by putting

$$V\propto I\propto E\propto \exp(\lambda t+ikz), \tag{9}$$

with $i^2=-1$, λ being a relaxation factor determined below, and k being the spatial mode. From the solvability condition that the determinant of the coefficient matrix equals zero, the eigenvalue λ is given by the equation:

$$\begin{aligned}CL\lambda^3-[CL(k_2-dk^2)-CR-DLk^2]\lambda^2\\+[1+DRk^2-(CR+LDk^2)(k_2-dk^2)]\lambda\\+k_1-k_2-(DRk_2-d)k^2+DdRk^4=0.\end{aligned} \tag{10}$$

As shown in the Appendix, the approximate solution of this equation can be easily obtained:

$$\lambda_1\doteq -q/3p,\quad \lambda_2,\lambda_3\doteq (q/6p)\pm i\sqrt{3p}, \tag{11}$$

with

$$\begin{aligned}p&=[1+DRk^2-(CR+LDk^2)(k_2-dk^2)]/3CL-r^2/9,\\q&=[k_1-k_2-(DRk_2-d)k^2+DdRk^4]/CL-(p+r^2/9)r,\\r&=R/L-k_2+(D/C+d)k^2.\end{aligned} \tag{12}$$

Equation (11) implies that the solution is non-periodic for $p<0$ but is periodic for $p>0$. Since we are now interested in the periodic rise of the spatial pattern, the following discussion is limited to the case of $p>0$.

If we focus attention on the most drastic change in pattern, the most important property in Fig. 4 is the coexistence of the nearly homogeneous increase over the cell length and the spatial differentiation with a period of approximately 30 mm. It may be, therefore, sufficient to describe analytically these two developing modes. Although the mode with high spatial frequencies observed in some experiments (Ogata 1983; Coster et al. 1985) can be expressed by superposition of each mode, only the two main modes of homogeneous and 30-mm-period components are described here. Within the framework of this approximation, the electric potential satisfying $V=0$ at $t=0$ for the initial condition can be expressed by

$$\begin{aligned}V=V_0[&\cos\theta\exp(\lambda_1 t)-\exp(\lambda' t)\cos(\lambda'' t+\theta)]\\&\cdot[1+\alpha\cos(kz+\beta)],\end{aligned} \tag{13}$$

where V_0 is the measure of amplitude of potential, λ' $(=g/6p)$ and λ'' $(=\sqrt{3p})$ denoting the real and the imaginary parts of λ_2, respectively. The numerical parameters determining the weight of each term are θ, α and β.

The explicit values of p, q, k, θ, α and β are determined so that the spatial period, the temporal period and the time for rise observed in Fig. 4 can be expressed well. The surface electric potential in Fig. 4 is measured from the extracellular origin far from the cell (see Fig. 1); hence the potential decay is remarkable. To compare the theoretical result with the experimental data, therefore, V in Eq. (13) must be multiplied by the damping factor γ. Its value is determined in the form of γV_0 so as to express well the observed data. Figure 7 demonstrates the calculated result of γV using Eq. (13). It can be seen that the spatial pattern is formed with oscillation, as found in the experiments. The fact that the spatial pattern and the oscillation can be reproduced at the same time by the single mathematical model implies that both phenomena originate

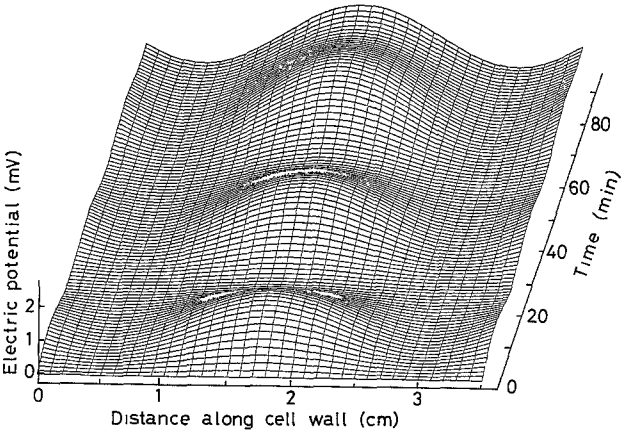

Fig. 7. Theoretical result of the electric pattern accompanying the oscillation. The numerical parameters are $p=1.23\times10^{-2}$ (1/min^2), $q=-1.05\times10^{-3}$ (1/min^3), $k=2.61$ (1/cm), $\theta=\pi/4$, $\alpha=1$, $\beta=5\pi/8$ and $\gamma V_0=1.1$ (mV). This result is compatible with the experimental observation in Fig. 4

in the same, or at least a similar, biochemical mechanism, although they have been observed separately in most cases of characean cells (Hansen 1978; Ogata 1983; Ogata and Kishimoto 1976). In other words, both the phenomena should be understood together as a spatio-temporal organization appearing far from equilibrium.

Discussion

Mechanism of electric spatial pattern formation in Chara

The increase of surface potential (Fig. 4) and the hyperpolarization (Ogata et al. 1987) occur along the entire cell length at the initial step of light illumination. The decrease in potential or the depolarization follows this event in a localized fashion; it leads to the electric differentiation. It is supposed that the light induces the H^+ efflux through the H^+-electrogenic process homogeneous over the cell. The resultant rise of surface potential or hyperpolarization with H^+ accumulation at the outer surface causes the subsequent H^+ influx (or OH^- efflux) according to the electrochemical gradient. If the influx can be balanced with the efflux at each point of the membrane, the homogeneous state along the cell is maintained.

A new state, however, can emerge when the light intensity is higher than some threshold (Toko et al. 1985, 1987a). This is partly due to a positive feedback mechanism where the membrane permeability to H^+ (or OH^-) increases at high pH (Bisson and Walker 1980; Bisson 1986). Furthermore, a positive feedback mechanism inherent to pump action assumed in the model (Toko et al. 1985), which is expressed by the second term k_2E on the RHS of Eq. (6), may also serve the banding (see Fig. 8). If the H^+ pump is activated through a signal from the chloroplasts (Hansen 1980, 1985), the equilibrium between HCO_3^- and CO_2 at position of H^+ efflux moves toward CO_2 production. Hence CO_2 diffuses into the cell (Walker et al. 1980; Lucas 1982), to be used in photosynthesis. As a result, the reaction steps in the chloroplasts are activated and this leads to further activated pump action. This process can be regarded as positive feedback, i.e., autocatalysis in terms of non-equilibrium thermodynamics. Addition of CO_2 made the pattern clearer (Lucas and Dainty 1977) but recent experiments have shown that the absence of CO_2 scarcely affects the pattern (Ogata et al. 1987). Thus the possibility of such a positive feedback must be examined further.

These positive feedback mechanisms are necessary conditions. The stable formation of bands requires a repressive factor too, such as competition between the spread of alkalinization due to passive flux and th spread of acidification due to active flux. This leads t

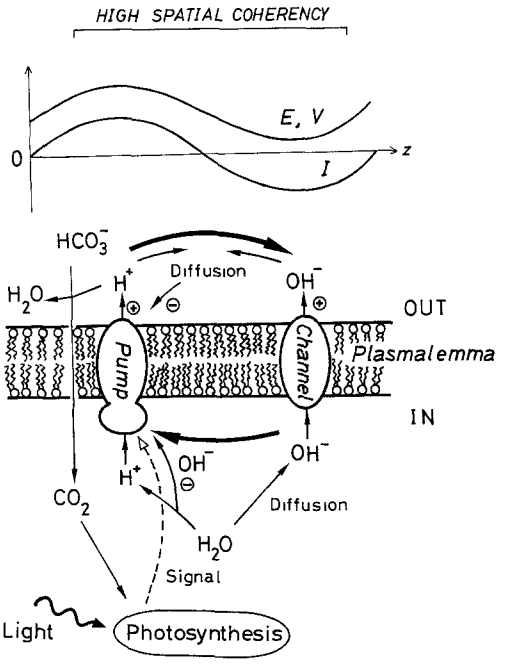

Fig. 8. Schematic illustration of spatial pattern formation in *Chara*. The symbols + and − imply the positive and negative feedbacks, respectively. The *thick solid lines* denote the electric current flowing between the acid and alkali regions. The calculated results (arbitrary units) are illustrated for the electromotive force E roughly expressing that of the electrogenic pump, the membrane potential V measured from the inside and the electric current I across the membrane. The H^+ pump is activated in a positive feedback way through CO_2 influx. The OH^- channel is also activated (Bisson and Walker 1980; Bisson 1986). It is probable that the signal from chloroplasts to the H^+ pump is the proton (Hansen 1980, 1985)

stabilization of the alternating band formation along the cell. The balance between neighbouring regions reflects a dynamic ordered state associated with ion flux, which can be observed as the electric current flowing between the acidic and alkaline regions. This is a kind of dissipative structure maintained through the electric current, which is proportional to the gradient of V in the present model. The electric current including diffusion is expressed by $-D\partial^2V/\partial z^2$ in Eq. (1) and internal diffusion is described by $-d\partial^2E/\partial z^2$ in Eq. (6). In Fig. 8, the profiles of E, V and I are also illustrated. The thick solid lines with arrows represent the electric current. The high coherency over a few centimetres results from diffusion-coupled membrane transport systems.

The possible biophysical steps are shown in Fig. 9. When the light is switched on, photosynthesis occurs. It dumps H^+ (or OH^-) as a signal to the cytoplasm (Hansen 1980, 1985); the H^+ pumps are activated. The relation between photosynthesis and pump action is the positive feedback through CO_2 influx, as above. process occurs uniformly over the entire cell . Thus, uniform hyperpolarization and an in-

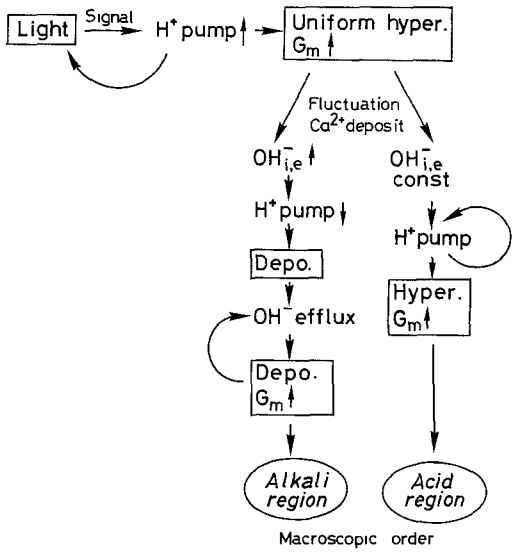

Fig. 9. Biophysical steps of spatial pattern formation in *Chara*. The experimental observation (Ogata 1983; Ogata et al. 1987) is shown by the *square*. The loops formed from two *arrows* show the positive feedback loops. The *arrows* ↑ and ↓ indicate increase (or activation) and decrease (or deactivation), respectively. Hyperpolarization is abbreviated by hyper and depolarization by depo. The intra- and extracellular OH^- concentrations are denoted by $OH^-_{i,e}$. G_m is the membrane conductance. It is important that microscopic fluctuations are amplified to the macroscopic level

crease in conductance are observed experimentally (Ogata 1983; Ogata et al. 1987). There always exist small fluctuations of the internal and external OH^- concentrations. If the OH^- concentration happens to increase at some position, the H^+ pump at this region may be weakened. It was reported that the pump current was decreased for internal alkalinization (Takeshige et al. 1986). It can be observed as a localized depolarization without conductance change (Ogata et al. 1987) or as a slight decrease in conductance (Ogata, personal communication). Outside the membrane, OH^- is accumulated more than in the neighbouring active pump regions. Inside the cell, depolarization causes an increase in OH^- concentration because of the electrochemical force, this leads to OH^- efflux. Thus the above behaviour of OH^- in the extra- and intracellular media bring about the depolarization and the conductance increase. This process is the positive feedback, as suggested (Bisson and Walker 1980; Bisson 1986). Stable alkaline regions are therefore formed.

In contrast, the regions where the OH^- concentration is kept almost constant show a quite different process. In these regions, the H^+ pumps are activated more. The hyperpolarization continues to grow (Ogata 1983; Ogata et al. 1987), to produce the stable acid regions.

In this way, initial fluctuations can increase to macroscopic levels. If calcium deposits exist, these regions can play a role as nucleation sites since OH^- may be already present. As can be seen from this explanation, the activation of the H^+ pumps is a leading factor (Hayashi et al. 1987). The positive feedback through OH^- in the alkaline regions can be considered as a stabilizing factor. This suggestion is supported by the fact that the differentiation of membrane potential occurs at an earlier stage than the change in conductance. The conductance in the alkaline regions becomes higher than in the acid regions after depolarization and hyperpolarization have settled down in these regions (Ogata et al. 1987; Ogata, personal communication). The resulting spatial pattern is highly cooperative temporally and spatially, as demonstrated by the coherent oscillation in Fig. 4 and the steady-state oscillation (Hayashi et al. 1987).

Let us here comment on the significance of the dissipative structure in characean banding. Firstly, it is clear that the structure of electrochemical inhomogeneity cannot be produced in the equilibrium state but is formed only under non-equilibrium conditions. As explained in Fig. 9, microscopic fluctuations increase to macroscopic levels; this can be observed experimentally as the acid/alkali banding. Although the bands appear to be static, they are really dynamic so as to generate self-oscillations. Secondly, the present theory suggests the existence of positive feedback in the electrogenic pumping process. While the feedback observed in OH^- efflux (Bisson 1986) is also necessary for the stabilization of bands, the major factor is the H^+-pump action. Thirdly, the balance between the acid and the alkaline bands can be explained by a competition between these regions through the electrochemical diffusion of H^+ (and OH^-), as illustrated in Fig. 8. These results can be obtained by considerations of the dynamic behaviour of the bands, i.e., dissipative structures.

An electric circuit model used in the present paper can simulate well the oscillatory rise of electric pattern. This model at present does not take account of the detailed electrophysiological structure of *Chara*. Nevertheless, it is noticeable that the simple theoretical model can describe the oscillatory spatial pattern. This is because the model is composed of three variables, V, I and E, which are described by the first derivative $\partial/\partial t$ in Eqs. (1), (2) and (6). As is well known, equations of two variables can only produce either the oscillation or the pattern near the thermodynamic equilibrium of weak non-linearity (Nicolis and Prigogine 1977). Therefore we can guess that the characean banding is a phenomenon related to the least three variables.

Self-organized state accompanying pattern formation and oscillation

Oscillations observed here may be considered as the appearance of the oscillatory component obtained

from the linearized response, i.e. the characteristic time τ_2, $\tau_3 = 3 \pm i \cdot 10\,\text{min}$ denoted by Hansen (1978). As can be seen from Eq. (8), the main contribution to the oscillation comes from the equation composed of two terms, $\partial^2 I/\partial t^2 + I/LC = 0$. This indicates the existence of a similar feedback to that previously suggested (Hansen 1980, 1985): The RHS of Eq. (8) describes the change in pH (because E is proportional to e) and the electric current due to the spatial potential difference. Thus Eq. (8) means a coupling between the fundamental oscillation of I, the internal pH and the inhomogeneous flux. It resembles a feedback loop suggesting previously (Hansen 1980, 1985) except for the inhomogeneous flux due to the formation of the spatial pattern.

The experimental observation in Fig. 4 shows that this oscillatory component appears along the entire cell length. It shows the existence of spatial coherency of the oscillation, which reaches over a few centimetres. In fact, the analysis using a cross-correlation function of steady self-oscillation revealed that the spatial coherency was very high in the acid region (Hayashi et al. 1987). These results may suggest that the pumping of H^+ is made cooperatively along the cell. This is apparent if we notice that H^+ pumping is an energy consuming process or a dissipative process maintained far from equilibrium. This concept concerning spatial correlation agrees with the result suggested in the usual pattern formation in chemical reaction systems with diffusion of ions (Lemarchand and Nicolis 1976). In this sense, the phenomenon found here in *Chara* resembles the propagation of the oscillatory wave found in the *Physarum plasmodium* (Matsumoto et al. 1986), which is interpreted as a self-organization phenomenon exhibiting the oscillation produced at each point of the cell. In multicellular systems such as the roots of beans, a similar oscillation with the formation of electric structure can be observed (Toko et al. 1986a, 1987b). In this case, too, oscillations frequently appear when a new pattern is added to the elongating root tip. Taking account of the fact that the oscillation can also appear in artificial membrane systems (Kamo et al. 1973; Kobatake 1975; Toko et al. 1986b), vectorial flow across the membrane seems to make the oscillation appear more readily.

The mathematical tools used here and in our previous papers (Toko et al. 1985) are similar to those adopted by Goodwin, who discussed pattern formation in *Acetabularia* in a mechanistic way (Goodwin and Trainor 1985). This kind of approach can be expected to be effective in elucidating the cooperation between transport molecules and cellular events leading to pattern formation.

Figure 4 shows that the phase of the oscillation is the same along the cell. It can, therefore, be considered that this oscillation is not the same as those oscillations connected with protoplasmic streaming found by Ogata and Kishimoto (1976); in the latter case the phase at one end of the cell is different from that at the other. These two kinds of oscillations are intimately related to the spatial electric inhomogeneity, and hence the phase at each point along the cell gives valuable information of spatio-temporal metabolic control in biological systems. It was reported that small signal oscillations and their phase correlation with conductance were light-dependent (Coster et al. 1985). The observation by Coster et al. that the phase spectrum shows phase correlations at lower temporal frequencies may agree with the present result.

Acknowledgements. We thank Dr. Koreaki Ogata in University of Occupation and Environmental Health for offering materials and giving valuable advice and helpful comments.

Appendix

Approximate solution of eigenvalues

Equation (10) is formally rewritten using r of Eq. (12) and p' and q', which correspond to the coefficients of Eq. (10):

$$\lambda^3 + r\lambda^2 + 3p'\lambda + q' = 0. \tag{A.1}$$

By transforming λ to $(\lambda - r/3)$, we can eliminate the term of the second power:

$$\lambda^3 + 3p\lambda + q = 0, \tag{A.2}$$

where p and q are given by Eq. (12). The solution λ is given by the following formula:

$$\lambda_1 = u + v, \quad \lambda_2 = u\omega + v\omega^*, \quad \lambda_3 = u\omega^* + v\omega, \tag{A.3}$$

where ω and ω^* (complex conjugate of ω) are the cubic roots of unity, with u and v given by

$$u^3 = [-q + (q^2 + 4p^3)^{1/2}]/2,$$
$$v^3 = [-q - (q^2 + 4p^3)^{1/2}]/2. \tag{A.4}$$

If we assume that q is much smaller than p, then u and v can be approximated by

$$u \doteq \sqrt{p}(1 - q/6p^{3/2}), \quad v \doteq \sqrt{p}(1 + q/6p^{3/2}). \tag{A.5}$$

The condition that $q \ll p$ holds near the transition point to bring about the appearance of the self-organized state. Since the light intensity is not far from the threshold level, it is adequate here.

Substitution of Eq. (A.5) into Eq. (A.3) leads to Eq. (11), where the displacement of λ, $-r/3$, is omitted because of the triviality of the simple change in the dc real component of λ. In Eq. (13) for the expression for V, the difference between λ in the $k = 0$ and $k \neq 0$ modes is neglected.

References

Bisson MA (1986) The effect of darkness on active and passive transport in *Chara corallina*. J Exp Bot 37:8–21

Bisson MA, Walker NA (1980) The *Chara* plasmalemma at high pH. Electrical measurements show rapid specific passive uniport of H^+ or OH^-. J Membr Biol 56:1–7

Boels HD, Hansen U-P (1982) Light and electrical current stimulate same feed-back system in *Nitella*. Plant Cell Physiol 23:343–346

Chilcott TC, Coster HGL, Ogata K, Smith JR (1983) Spatial variation of the electrical properties of *Chara:* II. Membrane capacitance and conductance as a function of frequency. Aust J Plant Physiol 10:353–362

Coster HGL, Chilcott TC, Ogata K (1985) Fluctuations in the electrical properties of *Chara* and the spatial structure of the electro-chemical characteristics. In: Lucas WJ, Berry JA (eds) Inorganic carbon uptake by aquatic photosynthesis organisms. The American Society of Plant Physiologists. Waverly Press, Baltimore, pp 255–269

Dorn A, Weisenseel MH (1984) Growth and the current pattern around internodal cells of *Nitella flexilis* L. J Exp Bot 35:373–383

Fisahn J, Mikschl E, Hansen U-P (1986) Separate oscillations of the electrogenic pump and of a K^+-channel in *Nitella* as revealed by simultaneous measurement of membrane potential and of resistance. J Exp Bot 37:34–47

FitzHugh R (1969) Mathematical models of excitation and propagation in nerve. In: Schwan HP (ed) Biological engineering, chapt 1. McGraw-Hill, New York

Fröhlich H (1983) Evidence for coherent excitation in biological systems. Int J Quantum Chem 23:1589–1595

Goodwin BC, Trainor LEH (1985) Tip and whorl morphogenesis in *Acetabularia* by calcium-regulated strain fields. J Theor Biol 117:79–106

Hansen U-P (1978) Do light-induced changes in the membrane potential of *Nitella* reflect the feed-back regulation of a cytoplasmic parameter. J Membr Biol 41:197–224

Hansen U-P (1980) Homeostasis in *Nitella:* Adaptation of H^+-transport to the photosynthetic load. In: Spanswick RM, Lucas WJ, Dainty J (eds) Plant membrane transport: Current conceptual issues. Elsevier North-Holland, Amsterdam, pp 587–588

Hansen U-P (1985) Messung und Interpretation der Kinetik der Lichtwirkung auf den elektrophoretischen Transport über die Plasmamembran der Alge *Nitella*. Ber Dtsch Bot Ges 92:105–118

Hayashi K, Fujiyoshi T, Toko K, Yamafuji K (1987) Periodic pattern of electric potential in *Chara* internodal cell. J Phys Soc Jpn 56:810–820

Kabashima S, Yamazaki H, Kawakubo T (1976) Critical fluctuation near threshold of Gun instability. J Phys Soc Jpn 40:921–924

Kamo N, Yoshioka T, Yoshida M, Sugita T (1973) Transport phenomena in a model membrane accompanying a conformational change. Transient processes in response to external stimuli. J Membr Biol 12:193–205

Kobatake Y (1975) Physicochemical problems in excitable membranes. Adv Chem Phys 29:319–340

Lemarchand H, Nicolis G (1976) Long range correlations and the onset of chemical instabilities. Physica 82 A:521–542

Lucas WJ (1982) Mechanism of aquisition of exogenous bicarbonate by internodal cells of *Chara corallina*. Planta 156:181–192

Lucas WJ, Dainty J (1977) HCO_3^- influx across the plasmalemma of *Chara corallina*. Plant Physiol 60:862–867

Lucas WJ, Nuccitelli R (1980) HCO_3^- and OH^- transport across the plasmalemma of *Chara:* Spatial resolution obtained using extracellular vibrating probe. Planta 150:120–131

Martens J, Hansen U-P, Warncke J (1979) Further evidence for the parallel pathway model of the metabolic control of the electrogenic pump in *Nitella* as obtained from the high frequency slope of the action of light. J Membr Biol 48:115–139

Matsumoto G (1981) Long-range spatial interactions and a dissipative structure in squid giant axons and a proposed physical model of nerve excitation. In: Matsumoto G, Kotani M (eds) Nerve membrane. University Tokyo Press, Tokyo, pp 203–220

Matsumoto K, Ueda T, Kobatake Y (1986) Propagation of phase wave in relation to tactic responses by the plasmodium of *Physarum polycephalum*. J Theor Biol 122:339–345

Nagumo J, Arimoto S, Yoshizawa S (1962) An active pulse transmission line simulating nerve axon. Proc IRE 50:2061–2070

Nicolis G, Prigogine I (1977) Self-organization in nonequilibrium systems. Wiley-Interscience, New York

Ogata K (1983) The water-film electrode: A new device for measuring the characean electro-potential and -conductance distributions along the length of the internode. Plant Cell Physiol 24:695–703

Ogata K, Kishimoto U (1976) Rhythmic change of membrane potential and cyclosis of *Nitella* internode. Plant Cell Physiol 17:201–207

Ogata K, Chilcott TC, Coster HGL (1983) Spatial variation of the electrical properties of *Chara australis*. I. Electrical potentials and membrane conductance. Aust J Plant Physiol 10:339–351

Ogata K, Toko K, Fujiyoshi T, Yamafuji K (1987) Electric inhomogeneity in membrane of characean internode influenced by light/dark transition, O_2, N_2, CO_2-free air and extracellular pH. Biophys Chem 26:71–81

Smith FA, Walker NA (1980) Effects of ammonia and methylamine on Cl^- transport and on the pH changes and circulating electric currents associated with HCO_3^- assimilation in *Chara corallina*. J Exp Bot 31:119–133

Smith JR, Walker NA (1983) Membrane conductance of *Chara* measured in the acid and basic zones. J Membr Biol 73:193–202

Smoes ML (1979) Chemical waves in the oscillatory *Zhabotinskii* system. In: Haken H (ed) Dynamics of synergetic systems. Springer, Berlin Heidelberg New York, pp 80–96

Spear DG, Barr JK, Barr CE (1969) Localization of hydrogen ion and chloride ion fluxes in *Nitella*. J Gen Physiol 54:397–414

Takeshige K, Shimmen T, Tazawa M (1986) Quantitative analysis of ATP-dependent H^+ efflux and pump current driven by an electrogenic pump in *Nitellopsis obtusa*. Plant Cell Physiol 27:337–348

Toko K, Nitta J, Urahama K, Yamafuji K (1981) Application of bifurcation theory to nerve excitations. Elect Commun Jpn 64A(9):1–10

Toko K, Iiyama S, Yamafuji K (1984) Band-type dissipative structure in ion transport systems with cylindrical shape. J Phys Soc Jpn 53:4070–4082

Toko K, Chosa H, Yamafuji K (1985) Dissipative structure in the *Characeae:* Spatial pattern of proton flux as a dissipative structure in characean cells. J Theor Biol 114:127–175

Toko K, Hayashi K, Yamafuji K (1986a) Spatio-temporal organization of electricity in biological growth. Trans IECE Jpn E69:485–487

Toko K, Tsukiji M, Iiyama S, Yamafuji K (1986b) Self-sustained oscillations of electric potential in a model membrane. Biophys Chem 23:201–210

Toko K, Fujiyoshi T, Ogata K, Chosa H, Yamafuji K (1987a) Theory of electric dissipative structure in characean internode. Biophys Chem 27:149–172

Toko K, Iiyama S, Tanaka C, Hayashi K, Yamafuji Ke, Yamafuji K (1987b) Relation of growth process to spatial patterns of

electric potential and enzyme activity in bean roots. Biophys Chem 27:39–58

Walgraef D, Dewel G, Borckmans P (1980) Fluctuations near nonequilibrium phase transitions to nonuniform states. Phys Rev A21:397–404

Walker NA, Smith FA (1977) Circulating electric currents between acid and alkaline zones associated with HCO_3^- assimilation in *Chara*. J Exp Bot 28:1190–1206

Walker NA, Smith FA, Cathers IR (1980) Bicarbonate assimilation by fresh-water charophytes and higher plants: I. Membrane transport of bicarbonate ions is not proven. J Membr Biol 57:51–58

Webb SJ, Thornton BS (1985) Dielectric structure and spatio-temporal organization in cells. Phys Scr 32:253–256

Yamafuji K, Toko K, Nitta J, Urahama K (1981) A reductive perturbation approach to hard-mode instabilities of inverted-type bifurcations. Prog Theor Phys 66:143–153